Surface acoustic wave propagation in graphene film

Article *in* Journal of Applied Physics · September 2015

DOI: 10.1063/1.4930050

11 authors, including:

Ivo Zizak
Helmholtz-Zentrum Berlin
97 PUBLICATIONS **1,655** CITATIONS
SEE PROFILE

Oleg V. Kononenko
Russian Academy of Sciences
75 PUBLICATIONS **346** CITATIONS
SEE PROFILE

Dmitrii Irzhak
Institute of Microelectronics Technology and …
79 PUBLICATIONS **246** CITATIONS
SEE PROFILE

Z. Insepov
Nazarbayev University
146 PUBLICATIONS **1,786** CITATIONS
SEE PROFILE

Surface acoustic wave propagation in graphene film

Dmitry Roshchupkin, Luc Ortega, Ivo Zizak, Olga Plotitcyna, Viktor Matveev, Oleg Kononenko, Evgenii Emelin, Alexei Erko, Kurbangali Tynyshtykbayev, Dmitry Irzhak, and Zinetula Insepov

Citation: Journal of Applied Physics **118**, 104901 (2015); doi: 10.1063/1.4930050
View online: http://dx.doi.org/10.1063/1.4930050
View Table of Contents: http://scitation.aip.org/content/aip/journal/jap/118/10?ver=pdfcov
Published by the AIP Publishing

Surface acoustic wave propagation in graphene film

Dmitry Roshchupkin,[1,a)] Luc Ortega,[2] Ivo Zizak,[3] Olga Plotitcyna,[1] Viktor Matveev,[1] Oleg Kononenko,[1] Evgenii Emelin,[1] Alexei Erko,[3] Kurbangali Tynyshtykbayev,[4] Dmitry Irzhak,[1] and Zinetula Insepov[4]

[1]*Institute of Microelectronics Technology and High-Purity Materials Russian Academy of Sciences, Chernogolovka 142432, Russia*
[2]*Laboratoire de Physique des Solides, Univ. Paris-Sud, CNRS, UMR 8502, 91405 Orsay Cedex, France*
[3]*Institute for Nanometre Optics and Technology, Helmholtz-Zentrum Berlin für Materialien und Energie GmbH, Albert-Einstein Strasse 15, 12489 Berlin, Germany*
[4]*Nazarbayev University Research and Innovation System, 53 Kabanbay Batyr St., Astana 010000, Kazakhstan*

(Received 21 May 2015; accepted 23 August 2015; published online 8 September 2015)

Surface acoustic wave (SAW) propagation in a graphene film on the surface of piezoelectric crystals was studied at the BESSY II synchrotron radiation source. Talbot effect enabled the visualization of the SAW propagation on the crystal surface with the graphene film in a real time mode, and high-resolution x-ray diffraction permitted the determination of the SAW amplitude in the graphene/piezoelectric crystal system. The influence of the SAW on the electrical properties of the graphene film was examined. It was shown that the changing of the SAW amplitude enables controlling the magnitude and direction of current in graphene film on the surface of piezoelectric crystals. © *2015 AIP Publishing LLC*. [http://dx.doi.org/10.1063/1.4930050]

I. INTRODUCTION

Modern acoustoelectronics is based on the surface and bulk acoustic waves. Today, acoustoelectronic devices are widely used in telecommunication systems where they allow the information processing and data transmission in a real time mode.[1] Acoustoelectronic devices are also widely used as physical quantity sensors, whose principle of operation is based on changing the resonance excitation frequency of acoustic waves under particular physical conditions (pressure, acceleration, temperature, humidity, etc.).[2–4]

Recently, an interesting proposal is the use of surface acoustic wave (SAW) in solar energy for acousto-stimulated transport of charge carriers generated by light in semiconductor structures.[5–8] The promising application of SAW in solar cells could increase their efficiency to 90%.[8] Surface acoustic wave propagating in piezoelectric crystals (GaN and GaAs including) possess opposite values of potential in SAW minima and maxima because of the piezoelectric effect. Electrons and holes sunlight-generated in a semiconductor structure are distributed between the SAW minima and maxima. The SAW then carries charges to the solar cell output at the velocity of the SAW. Using the SAW in solar cells would increase the area of charge collection in a semiconductor structure and increase the efficiency of solar cells.

Graphene opens up wider perspectives for solar power-engineering[9,10] where it can be used as a structure in which the electron-hole pairs are formed due to the radiation effect. Moreover, a graphene film is a good medium for SAW propagation. Several works reported the charge transfer by the SAW in graphene[11] and controlling the SAW amplitude by electric potential applied to a graphene film.[12]

This work presents the investigation of traveling SAW propagation in a graphene film on the surface of piezoelectric crystal by X-ray topography and diffraction at the BESSY II synchrotron radiation source. Another aim was to study the influence of the SAW amplitude on the acousto-stimulated transport of charge carriers in a graphene film.

II. SAW DEVICES WITH A GRAPHENE FILM

Crystals of lanthanum-gallium silicate group, langasite $La_3Ga_5SiO_{14}$ (LGS) and $Ca_3NbGa_3Si_2O_{14}$ (CNGS), were used to study the SAW propagation in a graphene film. These crystals, such as a piezoquartz crystal SiO_2, possess a point group symmetry 32 but, unlike SiO_2, have the high values of piezoelectric constants and electromechanical coupling coefficients.[13] Substrates from the crystal $Y-$ cut (planes (100) parallel to the crystal surface) were used to fabricate the SAW devices.

On the crystal surface, the interdigital transducer (IDT) was fabricated by photolithography to excite the SAW. The IDT consisted of 50 pairs of electrodes. On the $Y-$ cut of the LGS crystal the IDTs were fabricated to excite the SAW with the wavelength $\Lambda = 30$ μm at the resonance excitation frequency $f = 75.33$ MHz which propagated with the velocity $V = f \times \Lambda = 2260$ m/s along the X axis. The IDT on the $Y-$ cut of the CNGS crystal excited the SAW with the wavelength $\Lambda = 4$ μm at the resonance excitation frequency $f = 710$ MHz which propagated at $V = 2840$ m/s along the X axis.

The graphene film on the piezoelectric substrate surface between the two IDTs was formed by the transfer method.[14] First, the Ni film was deposited by the self-ion assisted deposition technique on the surface of an oxidized Si(100). The target was high purity Ni (99.9999%). Ion sputtering was performed in 10^{-6} Torr vacuum. The sputtered film thickness

a)Author to whom correspondence should be addressed. Electronic mail: rochtch@iptm.ru

was ~0.3 μm. The substrate with the sputtered Ni film was then placed in a quartz reactor tube pumped down to a pressure about 10^{-6} Torr and then inserted into a furnace preheated to 950 °C. When the samples were heated to the reaction temperature, acetylene was admitted into the quartz tube up to a pressure of 0.4 Torr for 5 s and then pumped out and the quartz tube reactor was extracted from the furnace.

Transfer of the resulting graphene was done with the aid of polymethylmethacrylate (PMMA) that was spincoated onto the surface of the graphene film to serve as a support. The PMMA/graphene layer was detached from the substrate by wet-etching of the Ni film with a 1% water solution of hydrochloric acid and then manually laid on the piezoelectric LGS (or CNGS) substrate between two IDTs. PMMA was then removed from the graphene surface by exposure to acetone in vapor and then liquid form.

Figure 1 shows Raman spectra of graphene measured after graphene synthesis on the Ni film and after its transfer onto the LGS piezoelectric substrate, respectively. The spectra were registered using the blue laser with the 488 nm wavelength at SENTERRA Raman microscope. The ratio of intensities of two peaks $I_{2D}/I_G \approx 2$ shows that the graphene film consists of 1–3layers of graphene.

To study the electric properties of graphene under the conditions of SAW propagation, two Al electrodes were formed on the graphene film surface by electron beam lithography. The distance between two electrodes was ~3 mm. Figure 2 shows the SAW devices with graphene which were used to examine the acoustic wave propagation in graphene films by X-ray topography and high-resolution X-ray diffraction and to investigate the influence of SAW propagation on the electrical properties of graphene.

III. TALBOT IMAGING OF THE SAW PROPAGATION IN A GRAPHENE FILM

X-ray diffraction on the acoustically modulated *Y*-cut of the LGS crystal was studied in the sagittal diffraction geometry in the scheme of a double-crystal x-ray diffractometer on the optical beamline KMC 2 at the BESSY II synchrotron radiation source. The experimental scheme is shown in Fig. 3. The X-ray wavelength $\lambda = 1.127$ Å ($E = 11$ keV) was selected with a Si(111) double-crystal monochromator which diffracts

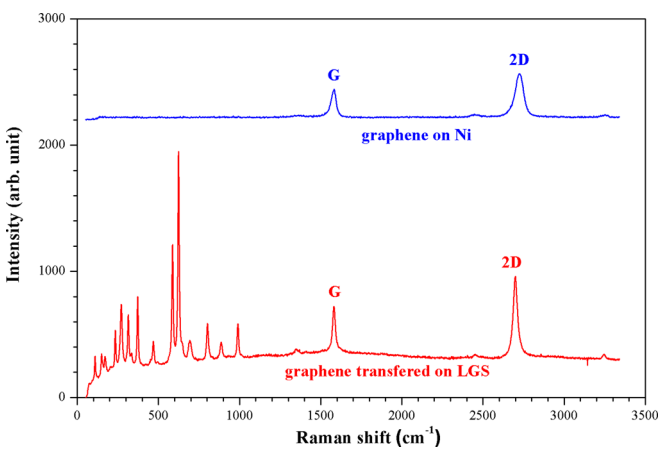

FIG. 1. Raman spectrum of graphene on Ni film and LGS substrate.

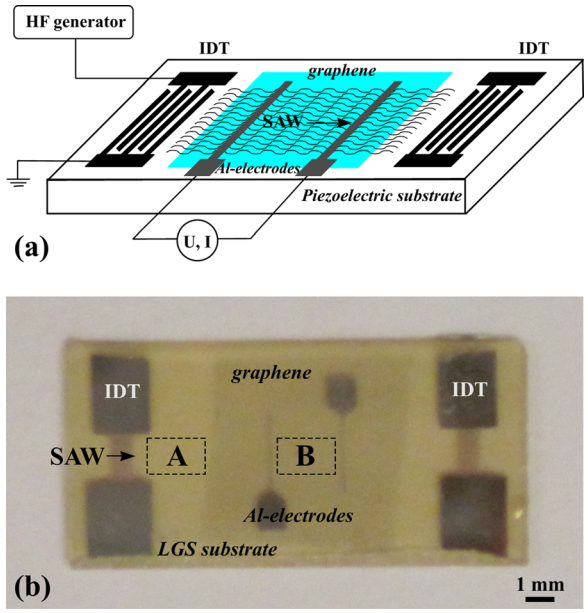

FIG. 2. SAW device with graphene: (a) scheme of SAW device, (b) photograph of SAW device.

X-ray radiation in a vertical plane. The LGS crystal modulated with a $\Lambda = 30$ μm SAW at the resonance excitation frequency $f = 75.33$ MHz was placed in the vertical plane so that the SAW wave vector was perpendicular to the X-ray wave vector. The reflection from the LGS plane (200) was used to visualize the SAW in the graphene film on the LGS crystal surface. X-rays at the Bragg incidence angle $\Theta_B = 9.168°$ to the studied LGS crystal diffract on the SAW serving as the diffraction grating for normal incidence in this diffraction geometry. SAW propagation in the crystal leads to sinusoidal modulation of a crystal lattice and, respectively, leads to sinusoidal modulation of a graphene film. SAW images were recorded with a CCD-camera with the pixel size of 0.645 μm. The SAW visualization is based on the Talbot effect. The Talbot effect consists in that the grating image is restored if the periodic grating is illuminated with a coherent radiation from a certain distance (the Talbot distance).[14,15] SAW is a strongly periodic grating and synchrotron radiation possesses a partially space-time coherence. In this case, an SAW image on the crystal surface can be observed at the Talbot distance ($Z_T = 2\Lambda^2/\lambda$, where Λ is the SAW wavelength and λ is the X-ray wavelength) or at the half of the Talbot distance ($Z_T/2$).[16]

Figure 4 presents an X-ray topograph of the *Y*-cut of the LGS crystal. The image corresponds to the free area A in Fig. 2(b). The reflection from the planes (200) at the Bragg angle $\Theta_B = 9.168°$ was used. The topograph displays an image of the acoustic wave field of $\Lambda = 30$ μm SAW. Figure 5 presents X-ray topographs from the surface of the crystal with graphene (area B in Fig. 2(b)) in the cases without modulation (a) and with modulation by the SAW (b). Without crystal surface acoustic modulation, the topograph exhibits boundaries of graphene blocks. Visualization of the graphene block boundaries was realized by the method of X-ray phase contrast in the optical scheme of Fig. 3,[17] because the LGS crystal, possessing a very narrow rocking curve,[18] can serve as a crystal-analyzer. In the optical scheme the graphene film

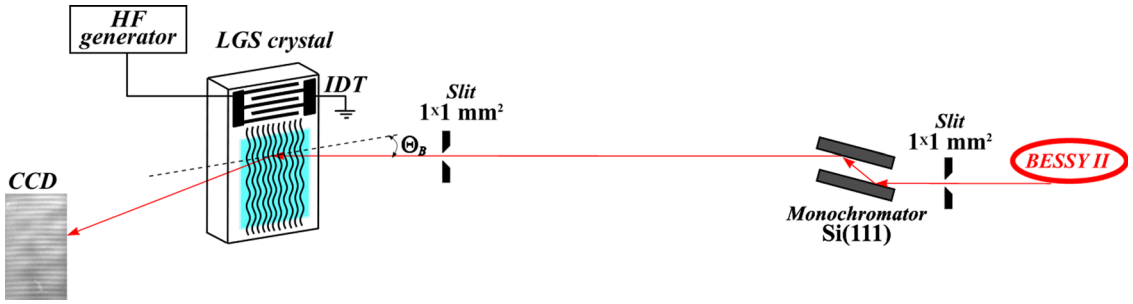

FIG. 3. Experimental setup of SAW imaging using Talbot effect.

was, correspondingly, positioned between the crystal-monochromator Si(111) and crystal-analyzer LGS(200).

Excitation of SAW enables to observe the SAW image on the crystal surface covered by graphene film (Fig. 5(b)). The topographs show that the presence of the graphene film on the crystal surface does not affect SAW propagation. The graphene film is only 1–3 monoatomic layers thick, which corresponds to a small weight load onto the crystal surface and does not cause changes in the SAW propagation velocity in the system graphene/crystal.

IV. X-RAY DIFFRACTION STUDY OF THE SAW PROPAGATION IN A GRAPHENE FILM

SAW propagation in the graphene film on the surface of the CNGS crystal was studied in the scheme of an X-ray double-crystal diffractometer schematically shown in Fig. 6. The wavelength of the X-ray used was $\lambda = 1.127$ Å ($E = 11$ keV). Primary and secondary slits with horizontal and vertical sizes 1×1 mm^2 and 60×60 μm^2, respectively, were used for X-ray collimation. A Cyberstar NaI scintillation detector with input slit size 60×60 μm^2 was used to record X-ray diffracted intensity. In this meridional diffraction geometry, the sinusoidal modulation of the crystal lattice by SAW serves as a Bragg diffraction grating and gives rise to diffraction satellites on the rocking curve. If the intensity of diffraction satellites is determined by the SAW amplitude, their angular divergence is determined as[19,20]

$$\delta\Theta_{mRC} = md/\Lambda, \tag{1}$$

where m is the diffraction satellite number номер, d is the interplanar spacing, and Λ is the SAW wavelength.

Figure 7 presents the results of investigation of X-ray Bragg diffraction on the system graphene/CNGS. The reflection from the (100) planes of the Y-cut of a CNGS crystal (interplanar spacing $d_{(100)} = 7.00953$ Å) at the Bragg angle $\Theta_B = 4.611^\circ$ was used for investigations. The SAW

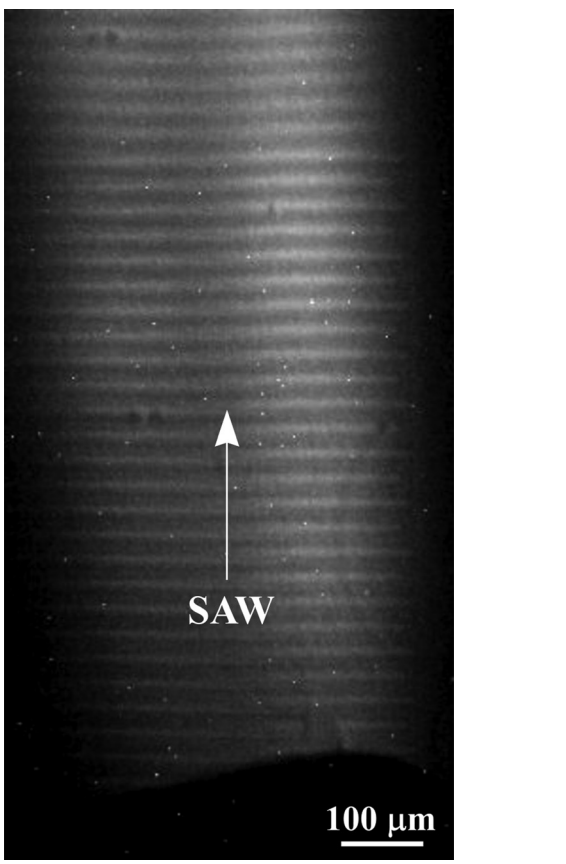

FIG. 4. X-ray topograph of the Y-cut of an LGS crystal excited by SAW in the region A of Fig. 2(b). $\lambda = 1.127$ Å; $\Lambda = 30$ μm; $f = 75.33$ MHz; reflection (200); $\Theta_B = 9.168^\circ$.

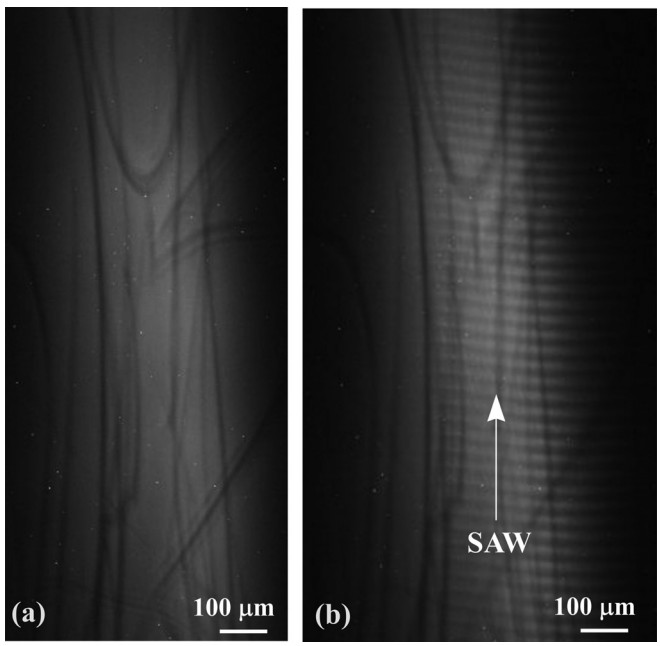

FIG. 5. X-ray topographs of the Y-cut of an LGS crystal in the region B of Fig. 2(b): (a) without SAW, (b) with SAW. $\lambda = 1.127$ Å; $\Lambda = 30$ μm; $f = 75.33$ MHz; reflection (200); $\Theta_B = 9.168^\circ$.

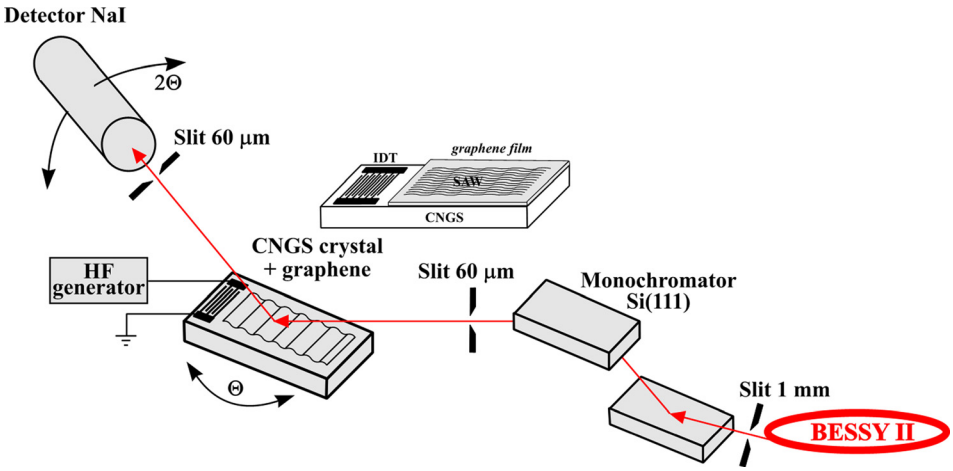

FIG. 6. Experimental setup of X-ray diffraction by SAW in CNGS crystal with graphene.

wavelength was $\Lambda = 4$ μm at the SAW resonance excitation frequency $f = 710$ MHz. The analysis of X-ray diffracted spectra and application of the kinematical model of X-ray diffraction enable an unambiguous determination of the SAW amplitude h on the crystal surface with a graphene film.[20,21]

Figure 7(a) displays the diffraction satellite intensities ($m = 0, \quad 1, \quad 2$) as the function of the amplitude of a high-frequency sinusoidal signal supplied to the IDT U.

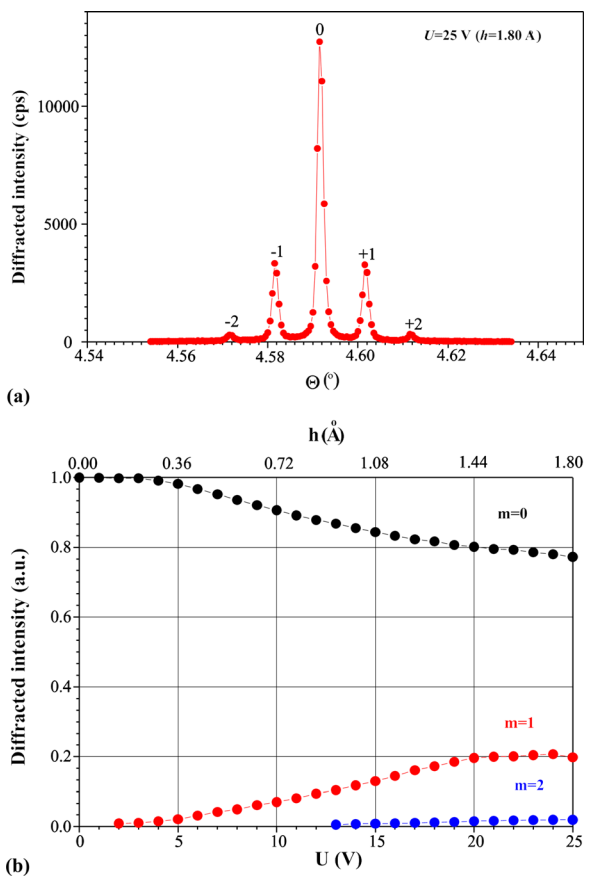

FIG. 7. X-ray diffraction by Y-cut of a CNGS crystal modulated by SAW: (a) intensities of the diffraction satellites vs. amplitude of the input signal supplied to the IDT U (vs. SAW amplitude h); (b) rocking curve measured at amplitude of the input signal supplied to the IDT $U = 25$ V (SAW amplitude $h = 1.80$ Å). $E = 11$ keV; reflection (100); $\Theta_B = 4.611°$; $\Lambda = 4$ μm; $f = 710$ MHz.

Diffraction satellites (except the zero diffraction satellite, $m = 0$) appear on the rocking curves at certain SAW amplitudes which increase with the increasing number of a diffraction satellite. The kinematical model of X-ray Bragg diffraction on acoustically modulated crystals permitted the determination of the SAW amplitude.[17–19] The SAW amplitude linearly depends on the amplitude of a high-frequency input signal supplied to the IDT. For example, the SAW amplitude is $h = 1.80$ Å at the amplitude of the input signal supplied to IDT $U = 25$ V.

Figure 7(b) shows the rocking curve measured at the amplitude of the signal supplied to IDT $U = 25$ V ($h = 1.80$ Å). The rocking curve exhibits two diffraction satellites on both sides of the intense Bragg peak. The intensity of the first diffraction satellite is ~20% of the Bragg peak intensity without SAW excitation. The high intensity of the Bragg peak is connected with a low absorption and a large penetration depth of X-ray radiation into the crystal, which considerably exceeds the depth of SAW propagation in the crystal. In this case, X-ray radiation diffracts both on the crystal lattice modulated by the SAW and on the crystal lattice deep in the crystal, which was not modulated by the SAW. The angular divergence between diffraction satellites on the rocking curve is $\delta\Theta_{mRC} = 0.010°$, which corresponds to calculated value from expression (1) for the SAW wavelength $\Lambda = 4$ μm.

V. MODULATION OF ELECTRIC PROPERTIES OF GRAPHENE BY SAW

Charge transport by SAW in the graphene film was studied using the Y-cut of the CNGS crystal on which surface a SAW propagates with the wavelength $\Lambda = 4$ μm at the velocity $V = 2840$ m/s along axis X. The graphene film was positioned between two IDTs and two Al-electrodes as shown in Fig. 2(b). The scheme of current measuring between two Al-electrodes is given in Fig. 2(a). The voltage applied to the electrodes was $U = 5$ mV. The current was measured at the SAW amplitude variation h from 0 to 1.80 Å and, correspondingly, variation of the amplitude of the input high-frequency signal U on the IDT from 0 to 25 V. Figure 8 displays the current dependence in the graphene film versus the SAW amplitude. The current in the graphene parabolically depends on the SAW amplitude because of the piezoelectric potential

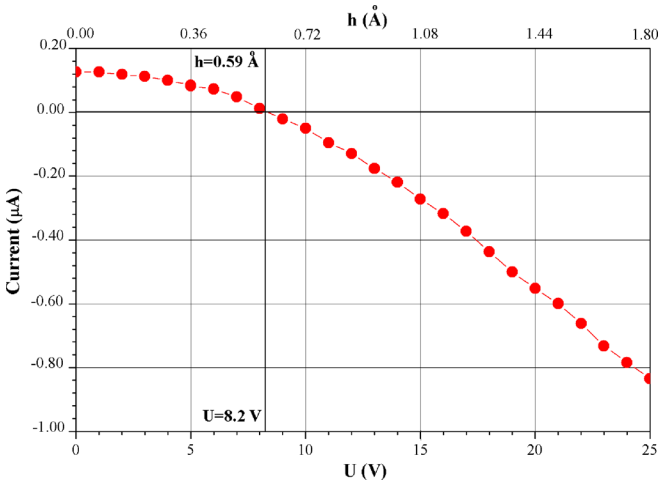

FIG. 8. Dependence of current in graphene vs. amplitude of the input signal supplied to the IDT U (vs. SAW amplitude h). $\Lambda = 4$ μm; $f = 710$ MHz.

between the SAW minima and maxima.[1] It is seen that the current decreases with an increasing of the SAW amplitude and at the SAW amplitude $h \approx 0.59$ Å the current becomes zero $I = 0$. At further growth of the SAW amplitude the current in the graphene film is observed to change its direction and increase between the Al-electrodes. At the SAW amplitude $h = 1.80$ Å, the current is $I = -0.84$ μA, which is 6.5 times higher than without SAW ($I = 0.13$ μA). The process is reversible and at a decrease of the SAW amplitude the current value returns to the initial value. Thus, variation of the SAW amplitude permits the value and direction of current to be controlled in a graphene film. This effect is determined by the SAW amplitude and consists in that a potential in the minima and maxima of the acoustic wave increases with the SAW amplitude growth and, correspondingly, the accumulation of charges in the graphene film and their transfer by SAW between the Al-electrodes increase too.

VI. CONCLUSION

Surface acoustic wave propagation in a graphene film on the surface of the Y-cut of LGS and CNGS crystals was studied on the synchrotron radiation source. Using the Talbot effect enables imaging of the SAW in the graphene film on the surface of the Y-cut of the LGS crystal in the real time mode. The X-ray phase contrast method revealed the block structure of the graphene film, which was formed on the surface of the piezoelectric substrate by the transfer method. The X-ray phase contrast method enabled the visualization of the block boundaries in the graphene film. It was shown that the block structure does not influence the SAW propagation in the system graphene/piezoelectric substrate, i.e., the block boundaries do not cause the SAW scattering.

The analysis of rocking curves of the SAW modulated system graphene/Y-cut of a CNGS crystal in terms of the kinematic model of X-ray diffraction allowed the determination of the values of the SAW amplitude. The possibility of controlling the current in the graphene film by operating the SAW amplitude was studied. It was shown that the value and direction of current in the graphene film can be controlled by changing the SAW amplitude. At a certain SAW amplitude value, charge transport in the graphene film can be completely suppressed (current is equal to zero).

The possibility of controlling the current in graphene is of interest for solar power engineering because acousto-stimulated transport of charge carriers can increase the efficiency of solar cells. Current control with SAW enables the creation of controllable devices, which would find application in micro- and nanoelectronics for the development of hybrid devices combining electric, optical, and acoustic properties. Furthermore, the acousto-stimulated transport of the charge carriers can be used in the future in semiconductor convolvers to control the properties of semiconductor diodes and transistors.[22] In the near future, a graphene film will be directly used in SAW devices for fabrications of IDT and SAW excitation in piezoelectric crystals.

ACKNOWLEDGMENTS

This work has been supported by the Ministry of Education and Science of the Russian Federation (Contract No. 14.607.21.0047, unique identifier No. RFMEFI60714X0047). D.R. is indebted to the Russian Foundation for Basic Research (Grant No. 14-02-91700) and to NUST "MISiS" (Grant No. K1-2015-046), K.T. and Z.I. are indebted to Nazarbayev University World Science Stars program (Grant No. 031-2013).

[1]C. Campbell, *Surface Acoustic Wave Devices and Their Signal Processing Applications* (Academic Press, San Diego, 1989).
[2]A. Pohl, IEEE Trans. Ultrason. Ferroelectr. Freq. Control **47**, 317 (2000).
[3]H. Fritze, H. L. Tuller, H. Seh, and G. Borchardt, Sens. Actuators, B **76**, 103 (2001).
[4]J. A. Thiele and M. Pereira da Cunha, Sens. Actuators, B **113**, 816 (2006).
[5]C. Rocke, S. Zimmermann, A. Wixforth, J. P. Kptthaus, G. Böhm, and G. Weimann, Phys. Rev. Lett. **78**, 4099 (1997).
[6]P. D. Batista, R. Hey, and P. V. Santos, Appl. Phys. Lett. **92**, 262108 (2008).
[7]S. J. Jiao, P. D. Batista, K. Biermann, R. Hey, and P. V. Santos, J. Appl. Phys. **106**, 053708 (2009).
[8]V. M. Yakovenko, Physica B **407**, 1969 (2012).
[9]K. S. Novoselov, A. K. Geim, S. V. Morozov, D. Jiang, M. I. Katsnelson, I. V. Grigorieva, S. V. Dubonos, and A. A. Firsov, Nature **438**, 197 (2005).
[10]M. I. Katsnelson and K. S. Novoselov, Solid State Commun. **143**, 3 (2007).
[11]V. Miseikis, J. E. Cunningham, K. Saeed, R. O'Rorke, and A. G. Davies, Appl. Phys. Lett. **100**, 133105 (2012).
[12]Z. Insepov, E. Emelin, O. Kononenko, D. V. Roshchupkin, K. B. Tnyshtykbayev, and K. A. Baigarin, Appl. Phys. Lett. **106**, 023505 (2015).
[13]M. P. da Cunda and S. A. Fagundes, IEEE Trans. Ultrason. Ferroelectr. Freq. Control **46**, 1583 (1999).
[14]H. F. Talbot, Philos. Mag. **9**, 401 (1836).
[15]L. Rayleigh, Philos. Mag. **11**, 196 (1881).
[16]D. Roshchupkin, L. Ortega, A. Snigirev, and I. Snigireva, Appl. Phys. Lett. **103**, 154101 (2013).
[17]F. Pfeiffer, T. Weitkamp, O. Bunk, and C. David, Nat. Phys. **2**, 258 (2006).
[18]D. V. Roshchupkin, D. V. Irzhak, R. Tucoulou, and O. A. Buzanov, J. Appl. Phys. **94**, 6692 (2003).
[19]R. Tucoulou, F. de Bergevin, O. Mathon, and D. Roshchupkin, Phys. Rev. B **64**, 134108 (2001).
[20]D. V. Roshchupkin, A. I. Erko, L. Ortega, and D. V. Irzhak, Appl. Phys. A **94**, 477–484 (2009).
[21]D. Irzhak and D. Roshchupkin, J. Appl. Phys. **115**, 244903 (2014).
[22]E. Dieulessant and D. Royer, *Ondes Elasfique dans les Solids* (Mason, Paris, 1974).